Macromolecules

Article

pubs.acs.org/Macromolecules

Kinetics of Two-Stage Dispersion Copolymerization for the Preparation of Lanthanide-Encoded Polystyrene Microparticles

Taunia L. L. Closson,[†] Chun Feng,[†] Adrienne Halupa, and Mitchell A. Winnik*

Department of Chemistry, University of Toronto, 80 St. George St, Toronto, ON, Canada M5S 3H6

Supporting Information

ABSTRACT: To obtain a better understanding of how lanthanide-encoded polystyrene microbeads are formed during their synthesis, we carried out kinetic studies of two-stage dispersion copolymerization of styrene and acrylic acid (AA, 2 wt % based on styrene), with or without added $TmCl_3$, in ethanol in the presence of poly(*N*-vinyl-2-pyrrolidone) (PVP) as a polymeric stabilizer. Particles of narrow size distribution and micrometer diameters were obtained, allowing us to compare rates of monomer conversion, Tm ion incorporation, and growth in particle size. In these reactions, AA or (AA + $TmCl_3$) were added in a second stage (t = 1 h). Much of the AA incorporation into the particles occurred in the latter half of the reaction. In the presence of small amounts of $TmCl_3$ there was some retardation of the polymerization reaction. The most striking result was that at the higher levels of $TmCl_3$ most of the metal ion incorporation occurred late in the reaction.

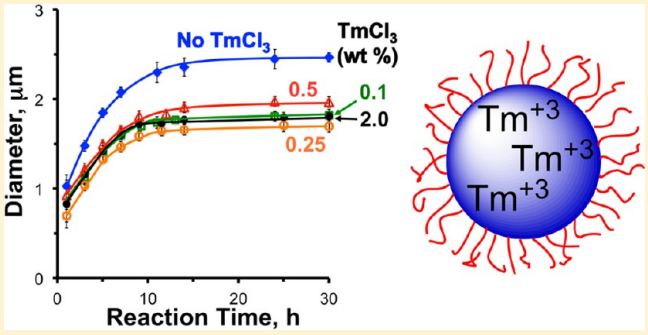

1. INTRODUCTION

Dispersion polymerization is a convenient way to synthesize polymer microbeads.[1−3] Invented in the UK in the 1960s,[4] this approach to particle synthesis received its biggest boost through the work of Lok and Ober[5] at Xerox in Canada in the 1980s on the radical polymerization of styrene in ethanol in the presence of hydroxypropyl cellulose (HPC). Dispersion polymerization is a type of precipitation polymerization in which a soluble monomer (e.g., styrene, St) is converted to an insoluble polymer (polystyrene, PS) in the presence of a polymeric stabilizer such as HPC that leads to the formation of colloidally stable particles. The impact of the work of Lok and Ober came from the fact that the particles they obtained had an exceptionally narrow size distribution. Over the next decade, there were many studies that explored the scope and mechanism of styrene dispersion polymerization in alcoholic media.[6−12] These studies established, for example, that both grafting and adsorption of poly(*N*-vinyl-2-pyrrolidone) (PVP) or other polymeric stabilizers to the growing particles were responsible for colloidal stability, but the grafting step was critical for successful polymerization reactions.[13]

Dispersion Copolymerization. One of the curious findings from these studies was that the reaction was not very tolerant to the presence of comonomers. Polymerizations could be carried out for monomer mixtures of styrene (St) and butyl acrylate (BA),[14−16] or in the presence of small amounts of acrylic acid (AA) or methacrylic acid (MAA).[17−19] Other comonomers, such as cross-linking agents or dye derivatives,[20,21] led to significant changes in particle size and the broadening of the particle size distribution.

In 2004, we reported a strategy for overcoming these difficulties. We hypothesized that the nucleation stage of the reaction was much more sensitive than the particle growth stage. For dispersion polymerization of styrene in ethanol, nucleation was shown to be over in a few minutes (less than 1% monomer conversion) after the start of the reaction.[12,22] Thus, if one delayed the addition of "problematic" comonomers until nucleation was complete, both particle size and its narrow size distribution could be maintained. This strategy works very well, particularly for the synthesis of cross-linked particles. We called this approach "two-stage" dispersion polymerization. Subsequent to our publication, we came across two earlier papers[20,23] that also reported that delaying the addition of a cross-linking agent to a dispersion polymerization reaction allowed the synthesis of uniform cross-linked polymer beads.

Over the intervening years, there have also been publications describing dispersion polymerization of methyl methacrylate (MMA) in water−alcohol mixtures.[18,24−26] When one reads these papers, one gets the sense that the nucleation stage for dispersion polymerization of MMA under these conditions may be less sensitive to perturbation by comonomers than corresponding polymerization reactions of styrene.

Recently, we have applied two-stage dispersion polymerization (2-Disp) to the synthesis of metal-encoded polystyrene microbeads. These beads were designed for bioanalytical applications such as bead-based immunoassays for bead-by-bead detection using mass cytometry. The particles were

Received: January 11, 2013
Revised: March 4, 2013
Published: March 18, 2013

   dx.doi.org/10.1021/ma400079q | *Macromolecules* 2013, 46, 2523−2534

synthesized by initiating styrene polymerization in ethanol in the presence of PVP and then, after about 5% styrene conversion, adding acrylic acid (AA) or methacrylic acid (MAA) in the presence of small amounts of lanthanide (Ln) salts.[27,28] These beads were shown to contain from 10^5 to 10^9 Ln ions per bead. To obtain a better understanding of the formation of these and obtain insights about the location of the metal ions within the particles, we have begun kinetic studies that examine in parallel monomer conversion, size evolution, and metal ion incorporation as the reaction proceeds. Before proceeding with a description of these experiments and our results, we first summarize previous studies of dispersion copolymerization.

Kinetic Studies of Dispersion Copolymerization. The experiments described in this section all examined batch ("one-stage") reactions, with all reactants added prior to initiation of polymerization. In the late 1990s, Lee and Seo[15] studied the dispersion copolymerization of St and BA in aqueous isopropanol with 2,2′-azoisobutyronitrile (AIBN) as the initiator and PVP as the stabilizer. They varied the monomer ratio (St/BA from 100/0 to 0/100), the initiator, the PVP, and the total monomer concentrations from 10 to 25 wt % as well as the reaction temperature (70−80 °C). They found that an increased St content led to an increase in polymerization rate and molecular weight of the final polymer, accompanied by a decrease in particle size. Other observations were consistent with previous findings on dispersion homopolymerization; for example, when the initiator concentration was increased, there was an increase in final monomer conversion and particle size,[2,3,7] and when the stabilizer content increased, the particle size decreased.[2,3] More interesting, as the particle size increased, the size distribution broadened.

Sáenz and Asua[14,16] studied the dispersion copolymerization of St and BA in ethanol/water with AIBN as the initiator, PVP as the stabilizer, and aerosol OT-100 (AOT-100: di-2-ethylhexyl ester of sodium sulfosuccinic acid) as an anionic surfactant. They varied the St/BA ratio from 100/0 to 55.2/44.8; the initiator content from 0.5 to 2.0 wt % and the PVP content from 0.5 to 2.0 wt % (both based on St); the ethanol/water ratio from 100/0 to 78/22; and the temperature from 53 to 69 °C. They found that solubility of the monomers and copolymers played an important role in the particle size and locus of polymerization. They found that the shift in the locus of polymerization from the continuous phase to the particle phase was more pronounced when particles were small and the solubility of the growing chains was low. They also showed that the reduction of the length of polymer chains was affected by an increase in ethanol content, and an increase in BA content, an increase in temperature, an increase in initiator content, and a decrease in stabilizer content. They also used their results to develop a mathematical model for dispersion copolymerization.

Several years later, Zhang et al.[20] studied the kinetics of AIBN-initiated dispersion copolymerization of St and the cross-linking agent divinylbenzene (DVB) in ethanol/water with PVP as the stabilizer. They varied the amount of St in the reaction mixture; the amount of DVB (0−4 wt % based on St); and the initial stabilizer content. They found that changes in the overall St content and the amount of DVB affected the particle size and broadened the size distribution. However, changes in the PVP content had no significant impact on the overall kinetics. They found that the polymerization at low St conversion occurred in the continuous phase and that the location of polymerization moved to the particles at higher St conversion. They also found that cross-linking (incorporation of the DVB monomer) was completed early in the reaction and was irregularly incorporated. They also reported that adding the DVB after 4 h of polymerization gave larger and monodisperse particles. However, for the late addition of DVB, they only studied the final particles and did not examine how this affected the reaction kinetics.

Other groups have examined dispersion copolymerization kinetics of MMA. Zhang et al.[18,24] studied the dispersion copolymerization in ethanol/water (with AIBN initiation, PVP stabilizer) of MMA and AA in the presence of ethylene glycol dimethyl acrylate (EGDMA) as a cross-linking reagent. They varied the ethanol/water composition (50/50 to 60/40), the weight ratio of MMA to AA (0.5/10 to 2.5/8.0), the temperature (63−70 °C), and the initiator concentration (1−5 wt % based on total monomer). The study focused mainly on the nucleation stage, but it was found that increasing the AA content resulted in a broadening of the particle size distribution.

Jiang et al.[25] studied the dispersion copolymerization of MMA and BA (AIBN initiation, PVP stabilizer) in methanol/water. They varied the BA content in the initial feed from 0 to 50 wt % and found that a higher fraction of MMA produced larger particles. They also found that the MMA polymerized preferentially early in the reaction, and BA polymerized more at the end of the reaction. The reaction rates for the copolymerization were lower than the homopolymerization of BA and were close to or lower than that of the homopolymerization of MMA.

Cockburn et al.[26] reported a study of the batch dispersion copolymerization of MMA and the biorenewable monomer γ-methyl-α-methylene-γ-butyrolactone (MeMBL). Reactions were carried out in methanol/water with 2,2′-azobis(2-methylbutyronitrile) (AMBN) as the initiator and PVP as the stabilizer. They varied the amount of MeMBL from 25% to 75% total monomer content and the methanol/water ratio from 60/40 to 80/20. They found that as they increased the MeMBL monomer content that both the particle size and the rate of polymerization decreased. When the volume of methanol was increased, the rate of polymerization decreased and the size of the particles increased. For all variations examined, they found a bimodal particle size distribution.

Kinetics of Two-Stage Dispersion Copolymerization. In the experiments described here, we carried out a series of kinetic studies of St polymerization in the presence of 2 wt % AA (based on St). To avoid any influence of the comonomer on the nucleation stage of the reaction, the AA or AA + lanthanide salts were added 1 h after the start of the reaction (ca. 10% St conversion). This addition step defines the start of the second stage of the reaction (t = 1 h). An initial measurement of St conversion was made at this point, but all subsequent measurements of conversion or lanthanide incorporation into the particles refer specifically to the second stage of the reaction. As will be seen below, these conditions led to the formation of uniform particles. Thus, we were able to compare the conversion of monomer, the uptake of lanthanide ions, and the evolution of particle growth throughout the various reactions.

2. EXPERIMENTAL SECTION

2.1. Reagents. Absolute ethanol, anisole (Aldrich, ≥99.7%), polyvinylpyrrolidone (PVP55) (Aldrich, M_w = 55 000 Da), Triton-X305 (TX305, 70% solution in water, Aldrich), styrene (St, Aldrich,

dx.doi.org/10.1021/ma400079q | Macromolecules 2013, 46, 2523−2534

99.9%), 2,2′-azobis(2-methylbutyronitrile) (AMBN, Dupont), thulium chloride hexahydrate ($TmCl_3 \cdot 6H_2O$, Aldrich, 99.99%), and acetonitrile (Aldrich, HPLC grade, ≥99.9%) were used without further purification. Water was purified through a Milli-Q purification system. High-purity HCl and HNO_3 for ICP-MS analysis were purchased from Seastar Chemical Inc. Acrylic acid (AA, Aldrich, 99%) was purified by distillation prior to storage under refrigeration at 4 °C.

2.2. Instrumentation. A Hitachi S-5200 field emission scanning electron microscope was used at operation voltages from 1 to 5 kV to measure particle size. Using the energy-dispersive X-ray spectroscope (EDX) (Inca, Oxford Instruments) attachment to a Hitachi HD 2000 transmission electron microscope (TEM), composition-based line scans were performed on relevant particles detected on the sample grid. The accelerating voltage for EDX measurements was 20 kV, and the current was 20 mA. Data were collected for a period of 10 min. The signal-to-noise ratio of the signal obtained was determined by considering the signal of an element known to not be present in the sample (e.g., La). EDX was used to determine incorporation of Tm ions into the particle interior and its distribution inside the beads.

The content of Tm in the supernatant was measured by an ELAN 9000 inductively coupled plasma mass spectrometer (PerkinElmer SCIEX) operating under normal Ar plasma conditions (1400 W forward plasma power, 17 L/min Ar plasma gas flow, 1.2 L/min auxiliary Ar flow, and 0.95 L/min nebulizer Ar flow). A cross-flow double pass spray chamber (PerkinElmer SCIEX) was employed in all instances. All the experiments were conducted using an autosampler (PerkinElmer AS 93) modified for operation with Eppendorf 1.5 mL tubes. Sample volume was fixed at 1.0 mL. The sample uptake rate was adjusted depending on the particular experiment, typically 100 μL/min. A standard solution was prepared from 1000 μg/mL PerkinElmer pure Single-Element Standard solution (PerkinElmer, Shelton, CT) by sequential dilution with high-purity HNO_3. Diluted high-purity HNO_3 (3%) was measured as a blank signal, which was subtracted from the sample signal. Then, the content of Tm in the supernatant was determined by normalizing the sample signals to the signal of the standard solution (1 ppb).

Mass cytometry measurements were performed with a CyTOF model C2 instrument from DVS Sciences (Markham, ON, Canada). The instrument is described in detail elsewhere.[29] Briefly, metal-encoded cells or polymer beads (in this work, Tm-encoded polystyrene microparticles) are introduced individually but stochastically into the plasma torch of an inductively coupled plasma mass spectrometer with time-of-flight detection (ICP-TOF-MS). Each resultant ion cloud produced by ICP is analyzed by TOF-MS through a dual counting, which is a combination of digital counting and analogue modes of ion detection, allowing simultaneous detection of very small and very large signals.

HPLC measurements were preformed with a PerkinElmer high-pressure liquid chromatography (HPLC) system (Waters, Symmetry C18 column, 5 μm, 4.6 × 150 mm). The UV detector (set at 205 nm) and column were at 23 °C. A water−acetonitrile mixture (v/v: 1/1) was used as the eluent with a flow rate of 1.0 mL/min. Anisole was used as an internal standard.

2.3. Dispersion Polymerization of Styrene with Acrylic Acid as a Comonomer. The recipe for the two-stage dispersion copolymerization of styrene with acrylic acid in ethanol is listed in Table 1. All of the stabilizer (PVP55), costabilizer (TX305), initiator (AMBN), the monomer (St), and ethanol were added to a 250 mL three-necked round-bottom flask equipped with a condenser, a mechanical stirrer connected to a polytetrafluoroethylene (PTFE) half-moon stirring paddle, and a gas inlet. The solution was deoxygenated by bubbling nitrogen for 30 min and stirred at 100 rpm. Aliquots (~0.5 mL) were collected from the reaction by microsyringe for HPLC analysis, and the flask was then placed in an oil bath preheated to 70 °C. The reaction time was measured once the solution was put into the preheated oil bath, and a nitrogen purge was maintained during the reaction. One hour after the polymerization reaction started (t = 1 h), an AA (or AA and $TmCl_3$) solution in ethanol was added into the reaction flask over around 1 min. The polymerization reaction was continued for 30 h, and aliquots (~0.5 mL) were taken from the reaction by a microsyringe at different time intervals. During the polymerization, each aliquot was analyzed by HPLC, ICP-MS, CyTOF, and SEM.

Table 1. Recipe for the Two-Stage Dispersion Copolymerization of St and AA in Ethanol

	two-stage reactions	
materials (g)	first stage	second stage[a]
styrene	6.27	
PVP(55000)	1.00	
TX-305	0.35	
AMBN	0.25	
ethanol	18.8	15.0
acrylic acid		0.13[b]
$TmCl_3 \cdot 6H_2O$		c

[a]1 h after the reaction was initiated. [b]2.0 wt % of comonomer AA based on the weight of St was added in each reaction. [c]Different levels of $TmCl_3 \cdot 6H_2O$ (0, 0.10, 0.25, 0.50, and 2.00 wt % based on the weight of St) were added in the second stage of the reaction.

2.4. Measuring the Conversion of Acrylic Acid and Styrene. The conversions of St and AA were determined by HPLC. A water−acetonitrile mixture (v/v: 1/1) was used as the eluent with a flow rate of 1.0 mL/min. Aliquots (100 μL) taken from the reaction at different time intervals were diluted with acetonitrile (4800 μL), and then a premixed anisole solution (100 μL, 1.0 mg/mL in acetonitrile) was added. The insoluble particles and polymers were removed by syringe filter (PTFE, pore size = 0.2 μm). Some of the filtrate solution was used to measure the concentration ratio of AA to anisole by HPLC to obtain the conversion of AA. In addition, 50 μL of the filtrate solution was diluted further with 300 μL of acetonitrile and 150 μL of a premixed anisole solution (1.0 mg/mL in acetonitrile) and analyzed by HPLC to obtain the concentration ratio of styrene to anisole to determine the conversion of St.

In these experiments, AA and $TmCl_3$ in ethanol (15.0 g) were added to the polymerization in the second stage (1 h after the initiation). Thus, the concentration of styrene was diluted compared to that in the first stage. To obtain a more precise measure of the dilution ratio, a control experiment was carried out. Styrene (6.25 g), AMBN (0.25 g), TX-305 (0.35 g), PVP (1.00 g), and ethanol (18.8 g) were added into a 250 mL three-necked flask, and the mixture was stirred for 15 min under nitrogen at room temperature. Then, 100 μL of the solution was taken from the mixture and diluted with acetonitrile (4800 μL) and 100 μL of a premixed anisole solution (1.0 mg/mL in acetonitrile). After AA (0.13 g), $TmCl_3 \cdot 6H_2O$ (12.5 mg) and ethanol (15.0 g) were added into the flask, and the mixture was stirred for another 10 min under nitrogen at room temperature; another 100 μL of solution was taken from the mixture and diluted with acetonitrile (4800 μL) and 100 μL of a premixed anisole solution (1.0 mg/mL in acetonitrile). The concentration ratio of styrene to anisole before and after adding AA, $TmCl_3$, and ethanol in the second stage were measured, and the result showed that the concentration of styrene after adding AA, $TmCl_3$, and ethanol was 0.664 times that of styrene at the first stage. This factor was used to compute the dilution of styrene to calculate its conversion at the start of the second stage of the reaction.

2.5. Characterization of Particle Sizes and Size Distributions. The bead diameters and diameter distributions were determined from images obtained with a Hitachi S-5200 FE scanning electron microscope (SEM). The samples for SEM were prepared by placing a drop of a diluted suspension on a Formvar/carbon-coated 200 mesh copper grid (Pelco). For each sample, average particle diameter (d_n) and particle size distribution were constructed on the basis of counting at least 200 individual particles in SEM images and analyzed by the software program ImageJ (National Institutes of Health). The particle size distribution was characterized in terms of coefficient of variation of particle diameter (CV_d):

dx.doi.org/10.1021/ma400079q | Macromolecules 2013, 46, 2523−2534

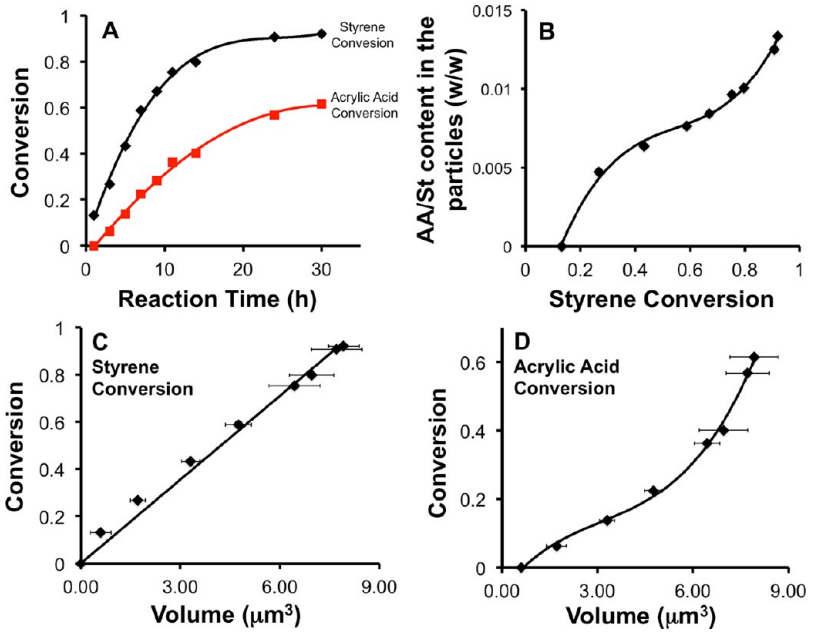

Figure 1. (A) Conversion of St and AA and (B) weight content of AA in the particles for the polymerization after adding 2.0 wt % of AA based on St in the second stage (t = 1 h). (C) Conversion of St and (D) conversion of AA versus particle volume for two-stage dispersion polymerization of St and AA. The x-axis represents the particle volume calculated from the diameter of the particle as measured by SEM, and the y-axis indicates the conversion of St and AA obtained by HPLC. AA was added 1 h after initiation, where particles were already formed with d_n = 1.03 μm at 0% AA conversion. The error bars show the standard deviation of the average volume calculated by measuring the diameters of ~200 particles.

$$CV_d = \frac{1}{d_n}\sqrt{\frac{1}{n-1}\sum_{i=1}^{n}(d_i - d_n)^2} \quad (1)$$

where d_i is the diameter of the ith particle and n is the total number of particles counted in the analysis.

2.6. Characterization of Tm Content by Mass Cytometry. The Tm content of the polystyrene particles was measured by mass cytometry. Aliquots of 100 μL were taken from each reaction, diluted with water, and washed with water twice by suspension and centrifugation. The washed particles were redispersed in water and diluted to ~10^6 particles/mL. The Tm content of polystyrene particles was determined by analyzing 20 000−30 000 individual particles. The number of Tm atoms per particle (N) was calculated using eq 2

$$N = I/T \quad (2)$$

in which I denotes the intensity value for each metal obtained by mass cytometry and T denotes the instrument transmission coefficient. The value of the transmission coefficient T represents the ratio of the number of ions detected by the TOF detector to the number of ions generated by the ICP torch, which is determined by instrument calibration using standard solutions of known metal concentration. For the current experiments, the value of T was 6.7 × 10^{-5} count/metal ion for ^{169}Tm.

2.7. ICP-MS. Aliquots (100 μL) taken from the reaction were diluted with 4900 μL of aqueous HNO_3 solution (3%) and spun down by centrifugation (13 000 rpm, 30 min) to obtain the supernatant. An aliquot (2.00 mL) of this clear solution was then transferred to a 5 mL of 3 kDa MWCO Millipore Amicon spin filter and centrifuged at 4000 rpm for 45 min. The flow-through solution was collected and diluted further with aqueous HNO_3 (3%) for ICP-MS analysis. The content of Tm ions in the supernatant was determined by normalizing the sample signals to the signal of the standard solution (1 ppb).

3. RESULTS AND DISCUSSION

In this work, we examine the kinetics of two-stage dispersion copolymerization of styrene and acrylic acid in ethanol at 70 °C in the absence or presence of varying amounts of $TmCl_3$. While the mechanism of dispersion homopolymerization is reasonably well understood, copolymerization introduces many complications. There is the difficulty common to all heterogeneous copolymerizations of the locus of the monomers and how that might change throughout the reaction.[30,31] In addition, comonomers can influence particle nucleation in ways that are very difficult to sort out.[24] Particle nucleation in dispersion polymerization is particularly sensitive. For example, even in a reaction as straightforward as dispersion homopolymerization of styrene in ethanol in the presence of PVP, particle nucleation is hard to control. Successive reactions run under seemingly identical conditions will all yield particles of very narrow size distribution, but the particle diameters of the different reactions are often different.[2] We examine two-stage dispersion polymerization as a means to avoid complications in particle nucleation caused by the presence of acrylic acid and lanthanide salts.[21,32] In our kinetics experiments, the moment of addition of the second stage monomer 1 h after initiation of the reaction defines time t = 1 h. We monitored the particle size by SEM and the conversion of St and AA by HPLC. When $TmCl_3$ was present in the reaction medium, we measured the amount of Tm^{3+} ions remaining in the reaction medium by ICP-MS and, in parallel, measured the bead-by-bead incorporation of Tm^{3+} ions into the particles by mass cytometry. One goal of our experiments was to understand the kinetics of the copolymerization of AA and St. A deeper goal was to learn about the timing of the incorporation of the Tm ions (a model lanthanide ion) with the hopes of generating mechanistic information to optimize future syntheses of Ln-encoded PS microbeads. All the experiments were carried out in ethanol in the presence of PVP of nominal molecular weight 55 000 (PVP55) plus Triton X-305 (TX305) as a costabilizer and initiated with AMBN.

3.1. Two-Stage Dispersion Polymerization of St and AA. *Monomer Conversion.* To begin, we examine the copolymerization of styrene with 2 wt % AA (based on styrene) added as an ethanol solution in the second stage. In

dx.doi.org/10.1021/ma400079q | Macromolecules 2013, 46, 2523−2534

Figure 1A, we plot St conversion and AA conversion vs reaction time beginning with the addition of AA to the reaction (t = 1 h). At the instant of AA addition, the St conversion had reached 13%. The St conversion increased relatively rapidly in the early stages of the reaction reaching 67% after 9 h. Subsequently, St conversion increased more slowly, 67% to 92%, as the polymerization continued another 21 h. Acrylic acid consumption was essentially linear with time for the first 12 h of the reaction and then began to level off, reaching only 62% after 30 h, when the reaction was ended. The less than complete conversion of monomer at 30 h is due to consumption of the initiator. The decomposition half-time of AMBN is ca. 6 h at 70 °C. At 10, 20 and 30 h after the initiation, approximately 31%, 9%, and 3% of AMBN, respectively, remained in the reaction.

To analyze these data, we assume that the monomer that was consumed in the reaction was incorporated into the particles. Thus, we can calculate the AA/St composition ratio of the particles as the reaction proceeds using the expression:

$$\frac{\text{AA}}{\text{St}}\ \text{content (w/w)} = \frac{\text{Conv(AA)} \times 2.0\%}{\text{Conv(St)}} \qquad (3)$$

where the term on the left-hand side of the equation is the weight ratio of AA/St and Conv(AA) and Conv(St) are conversion of AA and St, respectively. This ratio is plotted as a function of St conversion in Figure 1B. AA incorporation into the particles was rapid early in the reaction but increased only slowly between 25% and 70% St conversion. Toward the end of the reaction (70% to 92% St conversion), the AA content increased substantially. From these results we note that AA content increased most significantly at the end of the reaction.

If both monomers reacted exclusively in the continuous medium, we could use the known reactivity ratios for St and AA in alcoholic media (r_{AA} = 0.13 and r_{St} = 1.10 in methanol) to predict the relative rates of monomer conversion. These reactivity ratios indicate that St would add preferentially to the growing polymer chains in solution, influenced by the relatively small amount of AA present in the reaction. Complicating features are that this reactivity ratio is known to be sensitive to solvent polarity,[30,31,33] and one expects the St and AA to partition differently into the growing particles.

To proceed, we compare predicted values of St and AA conversions based on solutions to the Mayo–Lewis equations (4) and the reactivity ratios cited above, with the measured monomer conversions.

$$f_1 = 1 - f_2 = \frac{M_1}{M_1 + M_2}$$

$$F_1 = 1 - F_2 = \frac{r_1 f_1^2 + f_1 f_2}{r_1 f_1^2 + 2 f_1 f_2 + r_2 f_2^2} \qquad (4)$$

Here f_1 and f_2 are the mole fractions of styrene and acrylic acid, respectively, in solution, F_1 and F_2 are the mole fractions of these monomers in the copolymer, M_1 and M_2 are the number of moles of the monomers, and $r_1 = r_{St}$ and $r_2 = r_{AA}$ are the reactivity ratios. Details of the calculation are presented in the Supporting Information.

In Figure 2, we compare the measured amounts of monomer in solution as a function of total monomer conversion with the predictions of eq 4. For styrene, as the major monomer, it is not surprising (Figure 2A) that there is good agreement between the measured and predicted values. In fact, the styrene conversion results obtained here resemble data reported by

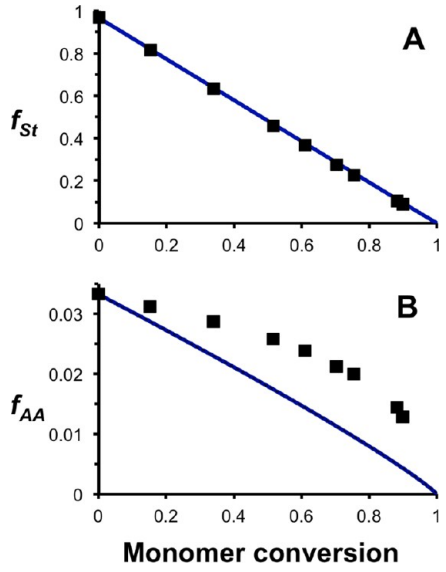

Figure 2. Predicted (—) and experimental (■) mole fractions of monomer in solution versus total mole conversion: (A) St and (B) AA. The amounts of St and AA used to calculate the predicted values are based on the amounts of St and AA at the start of the second stage (t = 1 h). The St was 13% of the initial amount of St at the start of the reaction (t = 0 h). The x-axis is the total mole conversion defined as the total moles of St and AA in the polymer over the total initial moles of St and AA.

the El-Aasser[6] group in 1988 on dispersion homopolymerization of styrene under conditions very similar to those employed here. They also examined the partitioning of styrene between the particle phase and the ethanol medium. The fraction of styrene in the particles went through a maximum at about 50% conversion but remained small throughout the reaction.

More interesting information is available for AA conversion (Figure 2B). One sees a buildup of AA monomer in solution over what would be predicted if the reaction had taken place entirely in solution. The most reasonable explanation for this difference is that much of the polymerization takes place in the particle phase, but the AA remains almost exclusively in the ethanol. Thus, there is relatively little polymerization of AA until the end of the reaction, when the amount of St is significantly reduced. One sees a sharp increase (in Figure 2B) in AA consumption once 90% of the styrene has reacted.

Particle Size Evolution. Figure 3 presents SEM images and diameter distribution histograms of the P(S-*co*-AA) particles at different times (3, 5, 14, and 30 h) after initiation of the reaction. For the sample collected at 3 h (Figure 3A–C), most of the particles had diameters (d) in the range from 1.3 to 1.6 μm with a CV_d of 4.0%, with a few small particles with $d \approx 0.7$ μm and some larger particles with d ranging from 1.8 to 2.4 μm. The number-average diameter (d_n) of the particles increased to 1.85 μm, with a CV_d of 2.8% after an additional 2 h as shown in Figure 3D–F. One can see that the number of smaller and larger particles (compared to the main population ranging from 1.7 to 2.0 μm) decreased. After polymerization for 14 h after the initiation, the average diameter of the particles evolved to 2.36 μm with a CV_d of 4.3% as shown in Figure 3G–I. Only a few smaller and larger particles (compared to the main population ranging from 2.2 to 2.5 μm) could be found. After 30 h reaction, d_n = 2.47 μm, with a CV_d of 2.1% as shown in Figure 3J–L.

dx.doi.org/10.1021/ma400079q | *Macromolecules* 2013, 46, 2523–2534

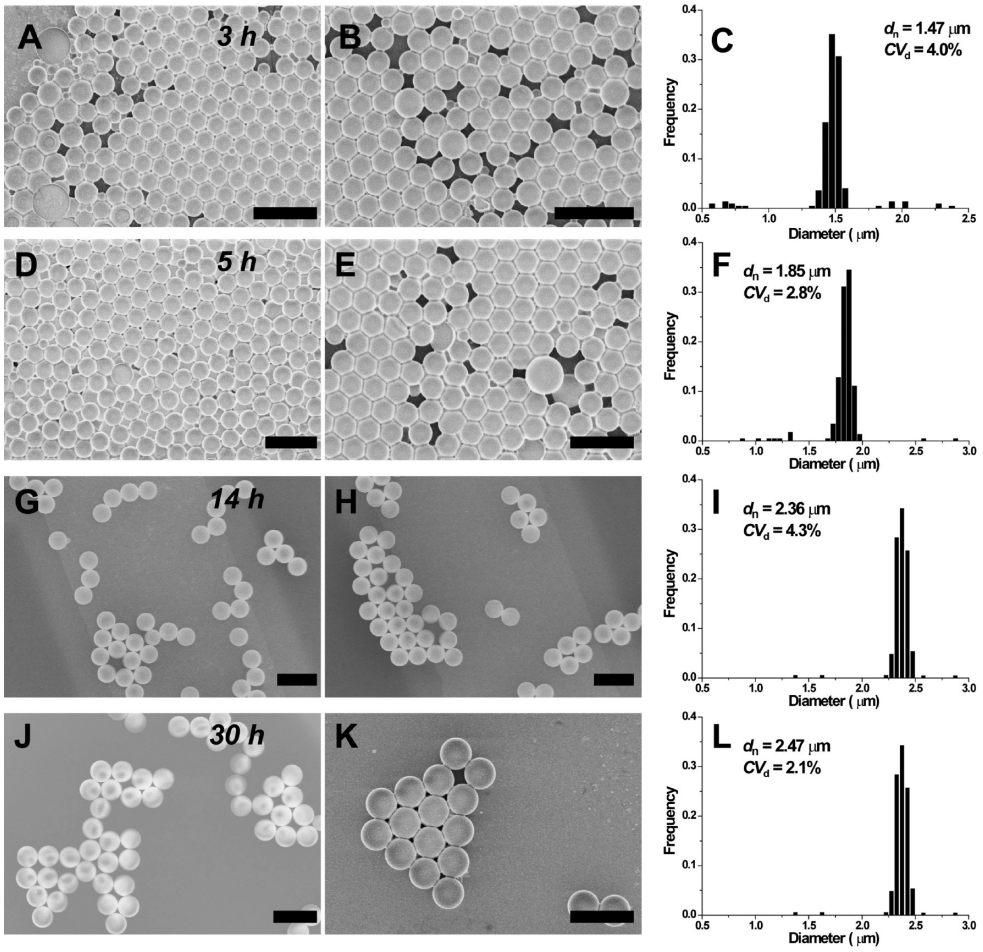

Figure 3. SEM images and diameter distribution histograms of the particles at different times after the initiation. This sample was synthesized by two-stage dispersion polymerization with PVP as the stabilizer in the presence of 2 wt % AA relative to the weight of styrene. 3 h (A, B, C); 5 h (D, E, F), 14 h (G, H, I); 30 h (J, K, L). Time zero refers to initiation of the reaction. The second stage reactants (AA) were added at t = 1 h. The scale bars are 5 μm.

The tiny amounts of small and large particles detected at low and intermediate styrene conversion are likely formed by precipitation of soluble polymer when the reactions were cooled from 70 °C to room temperature. We have observed this effect for two-stage dispersion polymerization of styrene in ethanol in the presence of chain transfer agents to reduce the molecular weight of the polymer in the particles.[34] Yasuda et al.[7] reported that the limiting molecular weight for PS solubility in ethanol at 70 °C is about 12 000. This value should increase for PS-*co*-PAA. We imagine that at high monomer conversion there is much less soluble polymer in the reaction that will precipitate as the solution is cooled. In this way, outliers in the particle size distribution disappear.

Figure S2 in the Supporting Information shows the evolution of the average particle diameter with time. Most of the particle growth occurred in the first 9 h of reaction. The particle size then leveled off, and the final average particle diameter was 2.47 μm. From d_n we can calculate the average volume of the particles.

Monomer Conversion and Particle Size. In Figure 1C,D we plot monomer conversion against particle volume. Figure 1C shows that styrene conversion tracks linearly with particle volume. If one assumes that the particles are composed only of PS (negligible amounts of AA, PVP, and TX305 content) and that all the St reacted ended up in the particles, then the linearity of this plot indicates that the number of particles in the reaction remained constant. No new particles were initiated as the reaction proceeded. On the basis of the value of the slope (slope = 0.12) obtained in Figure 1C, we calculated that the number of the particles obtained in this reaction was 1.42×10^{10} per mL. Calculations for this result and justification for assumption that AA, PVP, and TX305 make a negligible contribution to the particle volume are given in the Supporting Information. In Figure 1D, we see that the incorporation of AA increased late in the reaction, even after the particles had effectively stopped growing. This trend is similar to the growth in AA content of the particles plotted against the conversion of St.

3.2. Two-Stage Dispersion Polymerization in the Presence of Different Amounts of $TmCl_3$. Because of our interest in biomedical applications of Ln-encoded PS microbeads, we are particularly interested in understanding the factors that affect the timing and efficiency of lanthanide ion incorporation. Previous studies from our laboratory have found less than quantitative incorporation of Ln ions into PS particles in the presence of 2 wt % AA.[27] Another set of experiments on Ln incorporation into poly(styrene-*co*-methacrylic acid) (P(S-*co*-MAA)) microbeads,[28] we found high (>95%) incorporation levels when small amounts of $LnCl_3$ (0.1 wt % based on St) were introduced in the reaction. Higher

dx.doi.org/10.1021/ma400079q | *Macromolecules* 2013, 46, 2523−2534

amounts of $LnCl_3$ in the reaction (e.g., 0.5 wt %) led to lower ion incorporation into the particles. Here we use $TmCl_3$ as a representative lanthanide salt and examine reactions in which different amounts of $TmCl_3{\cdot}6H_2O$ (0.10, 0.25, 0.50, and 2.00 wt %) plus 2.00 wt % AA, all based on St, were added into the reaction 1 h after the initiation (t = 1 h). While these experiments could have been carried out with any lanthanide ion, Tm^{3+} offered two specific advantages. First, it consists of a single isotope, ^{169}Tm, and second, it has the highest atomic mass of the lanthanide elements. Both factors should enhance the sensitivity of determining metal ion incorporation into the particles, especially at early stages. The detector used in the mass cytometer is most sensitive to elements of higher atomic mass.

Monomer Conversion in Presence of Different Amounts of $TmCl_3$. In Figure 4, we present time−conversion plots for St and AA in the presence of different $TmCl_3$ concentrations. The overall shape of the plots resembles those in Figure 1A in the absence of Tm ions, but there appears to be a retardation of the reaction with increasing salt concentration. This conclusion is supported by the data in Table 2, which shows that the limiting monomer conversion (at 30 h reaction time) was significantly reduced, for example, from 92% to 78% for St and from 62% to 48% for AA in the presence of 2 wt % $TmCl_3$. We also note that there was some run-to-run variation in the extent of St conversion at 1 h reaction, when the AA and $TmCl_3$ were added.

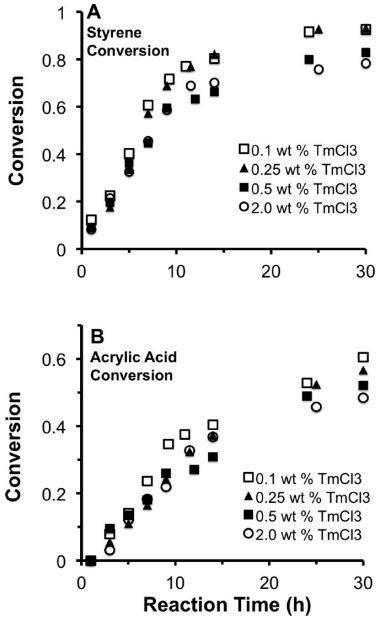

Figure 4. Conversion of St (A) and AA (B) for the polymerization with adding different amounts of $TmCl_3$ (0.10, 0.25, 0.50, and 2.00 wt % based on St) in the second stage (t = 1 h). The corresponding initial $TmCl_3$ concentrations were 0.4, 0.8, 1.7, and 6.6 mmol/L.

Figure 5 compares the AA content in the particle to that of St conversion during the polymerization in the presence of different amounts of $TmCl_3$. As in Figure 1B, these plots have a sigmoidal shape, but the presence of the $TmCl_3$ tends to exaggerate the plateau in AA content at about 50% St conversion.

Particle Size Evolution. The particle size evolution during the polymerization with the addition of different amounts of $TmCl_3$ was followed by SEM. We take the particle size evolution during the polymerization with 0.5 wt % of $TmCl_3$ as a representative example. These results are presented in Figure 6. Figures S4, S5, and S6 in the Supporting Information present the results for the other three samples prepared with different amounts of $TmCl_3$ (0.10, 0.25, and 2.00 wt %).

Table 2. Conversion of St at 1 h, Conversion of St and AA at 30 h, Final Particle Size, and Final Number of Particles per mL of Reaction Solution for Two-Stage Dispersion Polymerization in the Presence of Different Amounts of $TmCl_3{\cdot}6H_2O$

	1 h conversion	30 h conversion			
$TmCl_3{\cdot}6H_2O$[a] (wt %)	St (%)	St (%)	AA (%)	final particle diam (d_n, μm)	final no. of particles (10^{-10} × particles/mL)
0	13	92	62	2.47	1.42 ± 0.04
0.10	12	93	61	1.87	3.39 ± 0.04
0.25	9.4	93	57	1.70	4.05 ± 0.08
0.50	9.1	83	52	1.97	2.33 ± 0.04
2.00	8.4	78	48	1.81	2.87 ± 0.06

[a]Based on styrene. $TmCl_3{\cdot}6H_2O$ and AA were added to the reaction 1 h after initiation of the reaction.

Figure 6A,B shows the SEM images for the sample collected at 3 h after initiation of the reaction, and the histogram of diameters (d) is presented in Figure 6C. Although a few larger particles with a diameter about 3 μm were found, the diameter of the majority of the particles was located in the range from 1.15 to 1.35 μm with a CV_d of 5.1%. Two hours later, the average diameter of the particles increased to 1.81 μm, with a CV_d of 3.3% as shown in Figure 6D−F. A few large particles with $d \approx 3$ μm were still observed. After 14 h polymerization, the average diameter of the particles evolved to 1.91 μm with a CV_d of 3.1%, as shown in Figure 6G−I. Almost no particles around 3 μm could be found in the images we examined. Sixteen hours later, the average diameter of the particles increased to 1.97 μm, with a CV_d of 3.0% as shown in Figure 6J−L. At the beginning of the second stage of all five polymerizations, the PS particles formed had a relatively broad size distribution, and larger particles could be observed as shown in Figures 3A and 6B and in Figures S4B, S5B, and S6D. As mentioned above, we explain the presence of these in terms of precipitation of soluble polymer when the solutions were cooled from 70 °C to room temperature.

In Figure 7, we present a plot of particle size versus time. As the polymerization proceeded, the particle diameters (d_n) increased initially and then leveled off after about 9 h regardless of the content of $TmCl_3$ added in the second stage. While the final particle diameters appear to depend on amount of $TmCl_3$ in the reaction, another explanation is more likely. One should recall that the nucleation stage in dispersion polymerization is very short (less than 1% monomer conversion) but complex and highly sensitive to any small variation in reaction condition. Thus, the final size of the particles prepared by dispersion polymerization of styrene is difficult to control. Even two reactions that are conducted under seemingly identical conditions can give particles with somewhat different final particle sizes, both with a narrow size distribution.[2] We believe that the results in Figure 7 are a consequence of run-to-run variation in particle nucleation. This is the best way to explain

dx.doi.org/10.1021/ma400079q | Macromolecules 2013, 46, 2523−2534

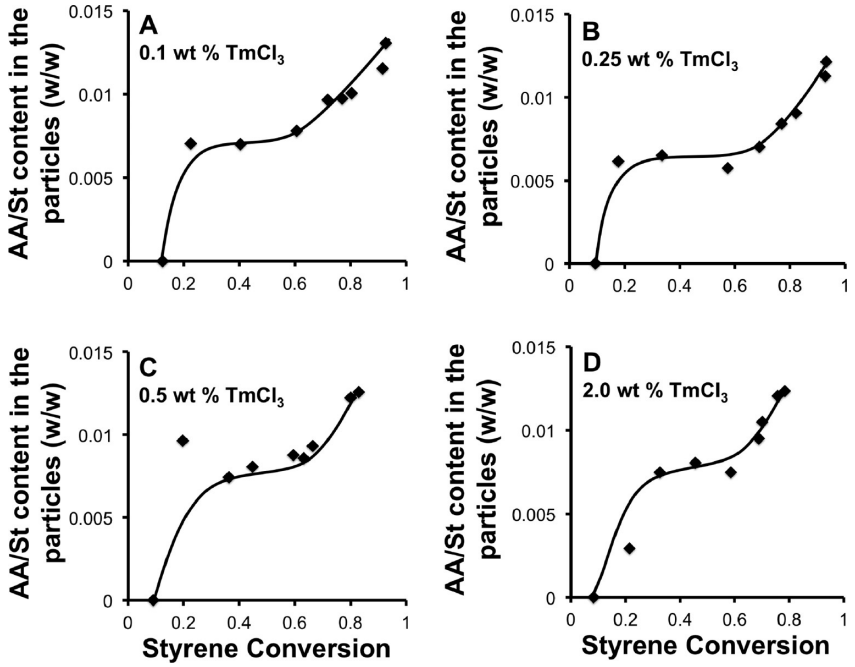

Figure 5. Evolution of the AA to St content in the particle during polymerizations carried out with (A) 0.10, (B) 0.25, (C) 0.50, and (D) 2.00 wt % of $TmCl_3 \cdot 6H_2O$ + 2.0 wt % AA based on St.

why the smallest particles were obtained in the reaction with 0.25 wt % $TmCl_3$.

Plots of St conversion against particle volume are presented in Figure S7. These plots are linear and consistent with the idea that no new particles formed as the reaction proceeded. From the slopes of these plots, we can calculate the number of particles formed in the reaction, which we report in Table 2 as particles/mL. A sample calculation for these results is given in the Supporting Information. Each reaction generates about 10^{10} particles/mL, and the reaction (0.25 wt % $TmCl_3$) that led to the smallest particle diameter produced the largest number of particles. This again is consistent with formation of a larger number of particles in the nucleation stage of this particular reaction. Plots of AA conversion vs particle volume are sigmoidal in shape (Figure S8) and resemble the plots in Figure 5 of AA content vs St conversion.

Evolution of Metal Ions per Particle Determined by Mass Cytometry and ICP-MS. In this section, we examine the rates at which Tm ions were incorporated into the PS particles. We employed two different analytical techniques. The Tm content of the particles was measured on a bead-by-bead basis by mass cytometry. In parallel, the residual Tm content of the continuous phase was measured by ICP-MS, after removing the particles by filtration. We assume in analyzing these data that any Tm ions not incorporated into the particles remain in the continuous phase.

We begin with the mass cytometry data, presented in Table 3. As the amount of $TmCl_3$ added in the second stage increased (0.10 to 2.00 wt %, based on St), the mean number of Tm ions incorporated increased from an average of 8.9×10^6 to 85×10^6 ions per particle. The final particle volume was different for each sample. Therefore, the number of Tm ions per particle obtained by mass cytometry did not directly reflect the influence of the Tm ion concentration on the reaction. To assess the influence of the amount of added Tm ions on the incorporation efficiency, we normalized these values by the final particle volume. In this way, we found that the number of Tm ions per unit volume increased from 2.8×10^6 to 27×10^6 ions/μm^3 as the amount of $TmCl_3$ in the reaction increased from 0.10 to 2.00 wt % based on St. This result shows that a 20-fold increase in the amount of $TmCl_3$ in the reaction led to only a 10-fold increase in Tm content in the particles. The values of Tm ions per μm^3 of particle volume did not increase linearly with the amount of $TmCl_3$ added during the polymerization. The Tm ion content per μm^3 of particle volume was lower than the value expected as more $TmCl_3$ was added. This observation indicates the incorporation efficiency decreased as more $TmCl_3$ was added during the polymerization.

In order to quantify the Tm incorporation efficiency, we measured the Tm content in the supernatant by ICP-MS. Associating the decrease of Tm content in the supernatant with Tm ions incorporated into the particles, we calculated that at the end of the reactions 89% of the metal ions added to the reaction with 0.10 wt % $TmCl_3$ (based on St) were present in the PS particles, whereas in the reaction with 2.0 wt % $TmCl_3$, only 52% of the metal ions became incorporated into the particles (Table 3). What we learn from these observations is that a higher content of $TmCl_3$ added in the second stage of the reaction led to a higher content of Tm per volume in the particles but at the same time resulted in a lower incorporation efficiency.

We next consider the kinetics of Tm ion incorporation into the particles. The Tm content of the beads was monitored as a function of monomer conversion by mass cytometry, and at the same time, the residual Tm ion content of the supernatant was monitored by ICP-MS. In Figure 8A, we plot the number of Tm ions per particle, and in Figure 8B, the percentage of Tm ions incorporated into the particles, both as a function of reaction time. Mass cytometry data were not available for reaction times less than 7 h because the Tm content in the particles was below the detection limit of the instrument.

For the particle synthesis with 0.10 wt % of $TmCl_3$, the number of Tm ions per particle reached 4.4×10^6 after 7 h polymerization and increased to 8.8×10^6 ions per particle at

dx.doi.org/10.1021/ma400079q | *Macromolecules* 2013, 46, 2523−2534

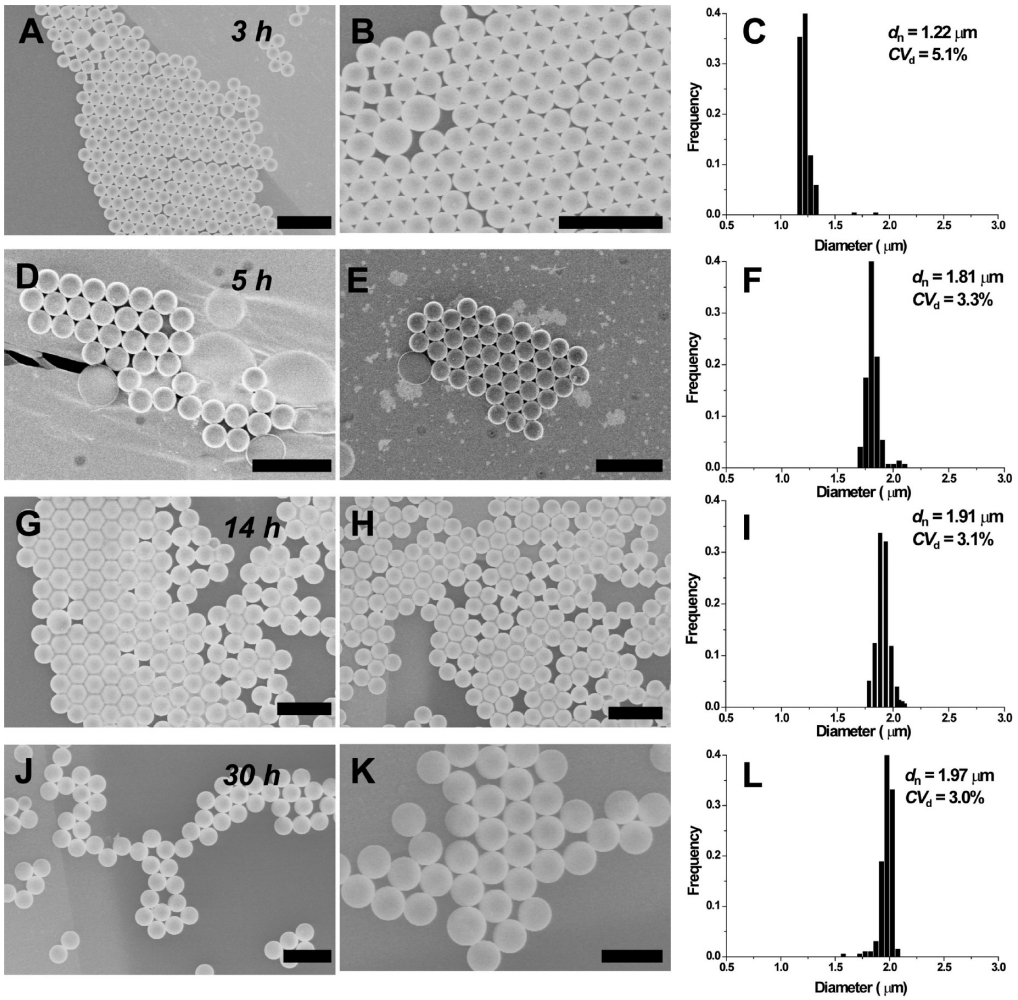

Figure 6. SEM images and diameter distribution histograms of the particle at different times after the initiation of the reaction. This sample was synthesized by two-stage dispersion polymerization with PVP as the stabilizer in the presence of 2.0 wt % AA, 0.50 wt % $TmCl_3$ relative to the weight of styrene. 3 h (A, B, C); 5 h (D, E, F); 14 h (G, H, I); 30 h (J, K, L). Time zero refers to initiation of the reaction. The second stage reactants (AA and $TmCl_3$) were added at t = 1 h. The scale bars are 5 μm.

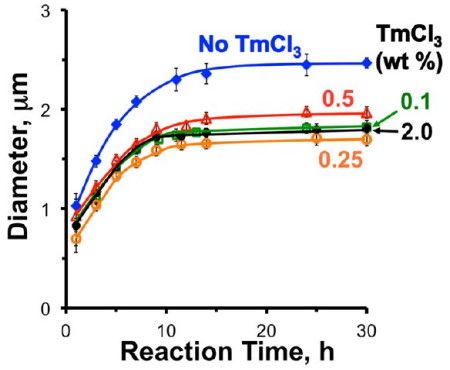

Figure 7. Evolution of the average particle diameter (d_n) with the polymerization time for the preparation of Tm-encoded PS particles. These samples were synthesized by two-stage dispersion polymerization with PVP as the stabilizer in the presence of 2 wt % of AA and 0, 0.10, 0.25, 0.50, and 2.00 wt % $TmCl_3$ based on St. The error bars show the standard deviation of d determined by measuring ~200 particle diameters per sample.

Table 3. Number of Tm ions per Particle, Number of Tm Ions per Particle Volume, and Tm Incorporation Efficiency at the End of the Reaction (30 h) for Different Levels of $TmCl_3$ Content

initial Tm content[a] (wt %) [(μmol)]	initial mole ratio of AA to Tm^{3+}	10^{-6} × Tm/bead[b] [CV]	bead vol[c] (μm^3)	10^{-6} × Tm/μm^3	incorporation[d] (%) [(μmol)]
0.10 [19]	97	8.9 [26%]	3.19	2.8	89 [17]
0.25 [41]	44	21 [21%]	2.60	8.1	83 [34]
0.50 [87]	23	46 [10%]	4.03	12	57 [49]
2.00 [328]	5.6	85 [11%]	3.14	27	52 [169]

[a]wt % $TmCl_3 \cdot 6H_2O$ based on styrene and [μmol $TmCl_3 \cdot 6H_2O$] in the reaction. The total reaction volume after addition of second stage reactants was 50 mL. [b]Average number of Tm ions per particle by mass cytometry [bead-to-bead variation in the Tm content]. [c]Average final particle volume (SEM). [d]Calculated from the amount of Tm ions in the reaction medium as measured by ICP-MS, with the assumption that what was not found in the reaction medium was in the particles.

13 h. It remained at this value as the polymerization continued over 30 h. The corresponding plot in Figure 8B indicates that 33% of the Tm ions in the initial reaction mixture of $TmCl_3$ became incorporated into the particles at 7 h reaction and increased to 81% at 13 h. At the end of the polymerization 89%

dx.doi.org/10.1021/ma400079q | Macromolecules 2013, 46, 2523−2534

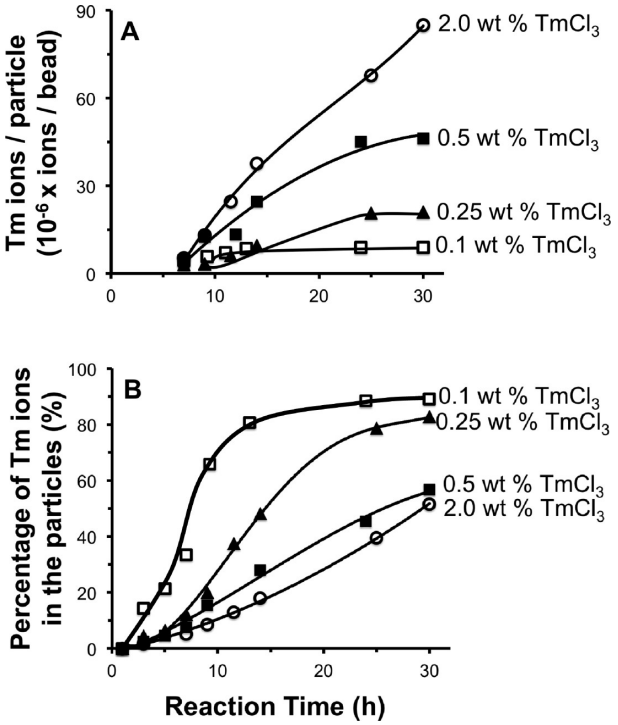

Figure 8. Change of Tm content of particle with the reaction time measured by (A) mass cytometry and (B) ICP-MS for reactions containing 2.00 wt % AA and different amounts of $TmCl_3$ (0.10, 0.25, 0.50, and 2.00 wt %) all based on St and added in the second stage of the reaction at t = 1 h.

of the Tm ions in the reaction were incorporated into the particles.

For the sample with 0.25 wt % $TmCl_3$, the number of Tm ions per particle was 3.0×10^6 at 7 h reaction, corresponding to 12% consumption the Tm ions added in the reaction. After 25 h, the number of Tm ions per particle increased to 21×10^6 (79% Tm ion incorporation; 83% at the end of the reaction). A similar Tm incorporation profile was observed for the sample with 0.50 wt % $TmCl_3$: the Tm ions content reached 4.1×10^6 ions per particle (7.6% incorporation efficiency) at 7 h and increased to 45×10^6 ions per particle (45% incorporation efficiency) at 24 h. The Tm ion content increased to 46×10^6 (57% incorporation efficiency) at the end of the reaction. For the reaction containing 2.00 wt % of $TmCl_3$, there was a pronounced increase in Tm content at the end of the reaction, with a significant increase between 24 and 30 h reaction, and no indication that this value was leveling off at the end of the polymerization.

Comparing Ion Incorporation with AA Consumption and with Particle Volume. Acrylic acid (or some other comonomer able to bind metal ions) is necessary for Ln ions to become incorporated into PS particles prepared by dispersion polymerization. Control experiments by Abdelrahman et al.[27] with $TmCl_3$ (0.1 wt % based on St) and a nearly identical combination of reactants showed that if AA was omitted from the reaction, negligible amounts of Tm ions ended up in the particles. In order to gain insights into how the AA comonomer facilitates Tm ion incorporation into the particles, we compare the increase in Tm content of the particles with the consumption of AA in the reaction. We are also interested in the locus of the Tm ions in the particles. As we show in Figure S10, EDX measurements do not have sufficient sensitivity to detect the relatively low levels of Tm ions incorporated into these particles. Some insights are possible, however, based on the timing of Tm ion incorporation in the reaction as described below.

In Figure 9A, we plot the number of Tm ions per particle determined by mass cytometry against the conversion of AA

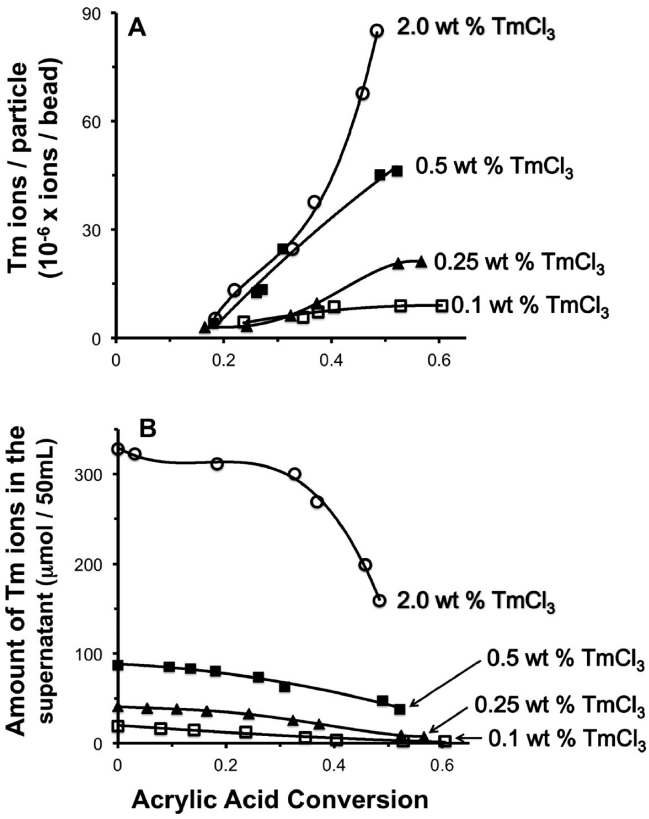

Figure 9. (A) Dependence of the content of Tm ions per particle and (B) the amount of Tm ions in supernatant on the conversion of AA during the particle synthesis with adding different levels of $TmCl_3$ (0.10, 0.25, 0.50, and 2.00 wt % based on St), but the same amount of AA (2.00 wt % based on St) in the second stage (t = 1 h). The Tm ions per particle were measured by mass cytometry, and the Tm ion content in the supernatant was measured by ICP-MS.

during the synthesis. In Figure 9B, we present the corresponding plot of the amount of Tm ions remaining in the supernatant. The striking feature for the two lowest amounts of $TmCl_3$ in the reaction is that ion incorporation is nearly complete when about 50% of the AA has reacted. In accord with the data in Figure 8, the residual Tm content of the continuous medium is very small.

For the particle synthesis with 0.50 wt % $TmCl_3$ [87 μmol per 50 mL reaction volume], no leveling off of Tm ion incorporation was observed. For this concentration of $TmCl_3$, the number of ions per particle appears to increase almost linearly with AA conversion until the end of the reaction, where the final conversion of AA was 52%. For the highest concentration of $TmCl_3$, the results are even more striking. Tm ion incorporation into the particles appears to accelerate with AA conversion as reflected both in the number of Tm ions per particle determined by mass cytometry and the decrease in Tm ion concentration in the supernatant determined by ICP-MS. For these two samples in particular, much of the metal ion incorporation takes place toward the end of the reaction. This

dx.doi.org/10.1021/ma400079q | *Macromolecules* 2013, 46, 2523−2534

result suggests that for these two samples a significant fraction of the metal ions are located near the surface of the PS particles.

Another way of gaining insights into the metal ion distribution in the particles is to examine how Tm ion incorporation varies with particle volume. In Figure 10, we plot

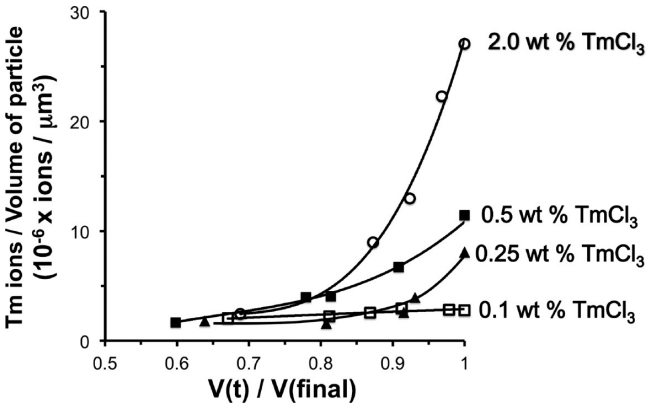

Figure 10. Content of Tm ions per volume of the particle synthesis with adding different levels of $TmCl_3$ (0.10, 0.25, 0.50, and 2.00 wt % based on St), but the same amount of AA (2.00 wt % based on St) in the second stage (t = 1 h) versus normalized volume of the particle.

Tm ions per unit volume in the particles against particle volume. To take account of the fact that particle size varied from reaction to reaction (Figure 7), we plot the metal ion content against the normalized growth in particle volume (volume at time t/final volume). The data show two rather different behaviors for the lowest and highest amounts of $TmCl_3$ in the reaction. For 0.1 wt % $TmCl_3$, the increase in Tm content is nearly linear across the reaction, suggesting that at this low level the Tm ions are uniformly incorporated into the particles. At the other extreme, for the highest amount of $TmCl_3$ in the reaction, most of the metal ions become incorporated toward the end of the reaction, during the last 10% of growth in particle volume. The reaction with 0.5 wt % $TmCl_3$ shows a similar behavior. These results are best explained by inferring that the Tm ions are located preferentially near the periphery of the PS particles.

4. SUMMARY AND CONCLUSIONS

We described kinetic studies of two-stage dispersion copolymerization of styrene (St) and acrylic acid (AA) in ethanol in the presence of PVP as a polymeric stabilizer. Additional experiments examined the influence of various amounts of $TmCl_3$ on the reaction as a model for understanding the synthesis of lanthanide-encoded PS microbeads intended for bioanalytical applications. The AA (2 wt % based on St or AA + $TmCl_3$) was added as a solution in ethanol 1 h after initiation of the reaction, corresponding to ca. 10% styrene conversion.

Particles with a narrow size distribution were obtained in every case, with diameters ranging from 1.5 to 2 μm. We attribute the variation in particle diameter to run-to-run differences in particle nucleation at early times in the reaction before the AA and $TmCl_3$ were added to the reaction. As one might expect, the growth in particle volume was proportional to styrene conversion, consistent with no new particles (i.e., no secondary nucleation) occurring as the reaction proceeded. For copolymerization of styrene with 2 wt % AA, the incorporation of AA into the particles was slower than one would anticipate, based on the reactivity ratios of the monomers assuming that polymerization occurred in the continuous medium. Much of the AA consumption took place in the later stages of the reaction, with about 40% of the AA unreacted at the end of the reaction.

In this reaction, one expects both monomers to reside primarily in the ethanol-rich solvent rather than in the particles. Results in the literature[6,11] for dispersion polymerization of styrene itself under very similar conditions showed that most of the unreacted styrene remained in the continuous phase during the entire reaction. AA, being more polar, should have an even smaller tendency to partition into the particles. Our results are consistent with the locus of polymerization occurring primarily in the growing particles, with some AA incorporation into the polymer throughout the reaction. Most of the AA became incorporated into the particles only after about 50% styrene conversion.

In the presence of small amounts of $TmCl_3$ (0.1−2.0 wt % based on St), there was some retardation of the reaction rate, accompanied by lower conversion of St and AA after 30 h reaction. Styrene conversion decreased from 92% in the absence of $TmCl_3$ to 78% in the presence of the highest amount of $TmCl_3$, and AA conversion decreased from 62% to 48%. As anticipated from previous experiments,[28] the number of Tm ions per particle ($\sim 10^6$ to $\sim 10^7$) increased with the amount of $TmCl_3$ added to the reaction, but the efficiency of Tm ion incorporation was lower for the reactions containing the larger amounts of $TmCl_3$. The most striking results were those associated with the timing of the Tm incorporation into the P(S-*co*-AA) particles. At 0.1 wt % $TmCl_3$, the metal ions became incorporated in the particles throughout the reaction, and by the end of the reaction, the residual Tm ion content of the supernatant was very small. For the higher amounts of $TmCl_3$, most of the metal ion incorporation occurred near the end of the reaction, suggesting that in this case most of the lanthanide ions were located near the surface of the particles. Electron microscopy experiments with EDX detection were not sensitive enough to detect the distribution of Tm ions in the particles.

We still have a rather poor understanding of the nature of the ion complexes that hold the lanthanide ions in these PS particles. We imagine that the metal ions are chelated to carboxyl groups incorporated into the polymer backbone. In this nonpolar PS environment, one might expect the ion chelates to cluster as one would find for a typical ionomer.[35] Lanthanide-encoded particles synthesized in this way are surprisingly resistant to ion leaching in water, even in the presence of common buffers including phosphate. When these particle dispersions are exposed to strong chelators such as ethylenediaminetetraacetic acid (EDTA), significant fractions of the Ln ions in the particles can be extracted into the aqueous phase.[36] These are the only other results that suggest that the Ln ions in the particle are located near the surface of the particles where they are accessible to the aqueous phase.

■ ASSOCIATED CONTENT

Supporting Information

Figures showing a sample HPLC curve measuring St and AA conversion; an evolution of d_n for two-stage dispersion polymerization of St and AA; ^{1}H NMR spectrum in CD_2Cl_2 of a PS particle sample; SEM images and size-distribution histograms for particles prepared in the presence of 0.1, 0.25, and 2.0 wt % $TmCl_3$; conversion of St vs particle volume for different $TmCl_3$ content; AA conversion vs normalized particle

dx.doi.org/10.1021/ma400079q | Macromolecules 2013, 46, 2523−2534

volume for different $TmCl_3$ content; a sample of gated and ungated Tm signal intensities for mass cytometry data; additional information including the calculation of the fraction of monomer in solution and in the copolymer; the calculation of the number of particles per reaction; the justification of assumption that AA, PVP, and TX305 make a negligible contribution to the size of the PS particles; the mass cytometry data acquisition; and EDX results. This material is available free of charge via the Internet at http://pubs.acs.org.

AUTHOR INFORMATION

Corresponding Author

*E-mail mwinnik@chem.utoronto.ca.

Author Contributions

†T.L.L.C. and C.F. made equal contributions to the work.

Notes

The authors declare no competing financial interest.

ACKNOWLEDGMENTS

The authors acknowledge NSERC Canada, the Province of Ontario, and DVS Sciences for their support of this research. We thank Dr. Mohsen Soleimani for helpful discussions throughout this project.

REFERENCES

(1) Arshady, R. *Colloid Polym. Sci.* **1992**, *270*, 717−732.
(2) Jayachandran, K. N. N.; Chatterji, P. R. *J. Macromol. Sci., Polym. Rev.* **2001**, 79−94.
(3) Kawaguchi, S. *Adv. Polym. Sci.* **2005**, *175*, 299−328.
(4) Barrett, K. E. J.; Thomas, H. R. *J. Polym. Sci., Part A: Polym. Chem.* **1969**, *7*, 2621−2650.
(5) Lok, K. P.; Ober, C. K. *Can. J. Chem.* **1985**, *64*, 209−216.
(6) Lu, Y. Y.; Vanderhoff, J. W.; El-Aasser, M. S. *J. Polym. Sci., Part B: Polym. Phys.* **1988**, *26*, 1187−1203.
(7) Paine, A. J.; Luymes, W.; McNulty, J. *Macromolecules* **1990**, *23*, 3104−3109.
(8) Baines, F. L.; Dionisio, S.; Billingham, N. C.; Armes, S. P. *Macromolecules* **1996**, *29*, 3096−3102.
(9) Ahmed, S. F.; Poehlein, G. W. *Ind. Eng. Chem. Res.* **1997**, *36*, 2597−2604.
(10) Ahmed, S. F.; Poehlein, G. W. *Ind. Eng. Chem. Res.* **1997**, *36*, 2605−2615.
(11) Lacroix-desmazes, P.; Guillot, J. *J. Polym. Sci., Part B: Polym. Phys.* **1998**, *36*, 325−335.
(12) Kim, J. W.; Kim, B. S.; Suh, K. D. *Colloid Polym. Sci.* **2000**, *278*, 591−594.
(13) Paine, A. J. *Macromolecules* **1990**, *23*, 3109−3117.
(14) Saenz, J. M.; Asua, J. M. *Macromolecules* **1998**, *31*, 5215−5222.
(15) Lee, K.-C.; Seo, H.-J. *Korea Polym. J.* **1998**, *6*, 405−413.
(16) Saenz, J. M.; Asua, J. M. *Colloids Surf., A* **1999**, *153*, 61−74.
(17) Li, G.; Zhang, Z. *J. Dispersion Sci. Technol.* **2004**, *25*, 83−88.
(18) Zhang, H.; Huang, H.; Lv, R.; Chen, M. *Colloids Surf., A* **2005**, *253*, 217−221.
(19) Tseng, C. M.; Lu, Y. Y.; El-Aasser, M. S.; Vanderhoff, J. W. *J. Polym. Sci., Part A: Polym. Chem.* **1986**, *24*, 2995−3007.
(20) Zhang, H. T.; Huang, J. X.; Jiang, B. B. *J. Appl. Polym. Sci.* **2002**, *85*, 2230−2238.
(21) Song, J.; Tronc, F.; Winnik, M. A. *J. Am. Chem. Soc.* **2004**, *126*, 6562−6563.
(22) Yasuda, M.; Seki, H.; Yokoyama, H.; Ogino, H.; Ishimi, K.; Ishikawa, H. *Macromolecules* **2001**, *34*, 3261−3270.
(23) Horak, D.; Karpisek, M.; Turkova, J.; Benes, M. *Biotechnol. Prog.* **1999**, *15*, 208−215.
(24) Zhang, H.-T.; Yuan, X.-Y.; Huang, J.-X. *React. Funct. Polym.* **2004**, *59*, 23−31.
(25) Jiang, S.; Sudol, E. D.; Dimonie, V. L.; El-aasser, M. S. *J. Polym. Sci., Part A: Polym. Chem.* **2007**, *45*, 2105−2112.
(26) Cockburn, R. a.; McKenna, T. F. L.; Hutchinson, R. A. *Macromol. React. Eng.* **2011**, *5*, 404−417.
(27) Abdelrahman, A. I.; Dai, S.; Thickett, S. C.; Ornatsky, O.; Bandura, D.; Baranov, V.; Winnik, M. A. *J. Am. Chem. Soc.* **2009**, *131*, 15276−83.
(28) Liang, Y.; Abdelrahman, A. I.; Baranov, V.; Winnik, M. A. *Polymer* **2011**, *52*, 5040−5052.
(29) Bandura, D. R.; Baranov, V.; Ornatsky, O.; Antonov, A.; Kinach, R.; Lou, X.; Pavlov, S.; Vorobiev, S.; Dick, J. E.; Tanner, S. D. *Anal. Chem.* **2009**, *81*, 6813−6822.
(30) Kim, S. Effect of solvent on free radical initiated copolymerization of styrene and acrylic acid. Akron University, 1990; pp 1−139.
(31) Borisova, O.; Billon, L.; Zaremski, M.; Grassl, B.; Bakaeva, Z.; Lapp, A.; Stepanek, P.; Borisov, O. *Soft Matter* **2012**, *8*, 7649.
(32) Song, J. S. Synthesis and Characterization of Monodisperse Functionalized Micron-Size Polymeric Microspheres by Two-Stage Dispersion Polymerization. University of Toronto, 2006.
(33) Zhao, Y.; Dar, Y. L.; Caneba, G. T. *Ind. Eng. Chem. Res.* **2008**, *47*, 3568−3581.
(34) Song, J.-S.; Winnik, M. A. *Polymer* **2006**, *47*, 4557−4563.
(35) Eisenberg, A.; Hird, B.; Moore, R. B. *Macromolecules* **1990**, *23*, 4098−4107.
(36) Liang, Y.; Abdelrahman, A. I.; Baranov, V.; Winnik, M. A. *Polymer* **2012**, *53*, 998−1004.